

Supporting Information

## **Binary cooperative flexible magnetoelectric materials working as self-powered tactile sensors**

Xuan Zhang,<sup>†a,c</sup> Jingwei Ai,<sup>†a</sup> Zheng Ma,<sup>†a</sup> Zhuolin Du,<sup>a</sup> Dezhi Chen,<sup>b</sup> Ruiping Zou,<sup>c</sup>

Bin Su<sup>\*a</sup>

<sup>a</sup>State Key Laboratory of Material Processing and Die & Mould Technology, School of Materials Science and Engineering, Huazhong University of Science and Technology, Wuhan 430074, Hubei, P. R. China,

<sup>b</sup>State Key Laboratory of Advanced Electromagnetic Engineering and Technology, School of Electrical and Electronic Engineering, Huazhong University of Science and Technology, Wuhan 430074, Hubei, China,

<sup>c</sup>ARC Hub for Computational Particle Technology, Department of Chemical Engineering, Monash University, Clayton VIC 3800, Australia.

\* To whom correspondence should be addressed: B. Su. ([subin@hust.edu.cn](mailto:subin@hust.edu.cn))

† These authors contributed equally to this work.

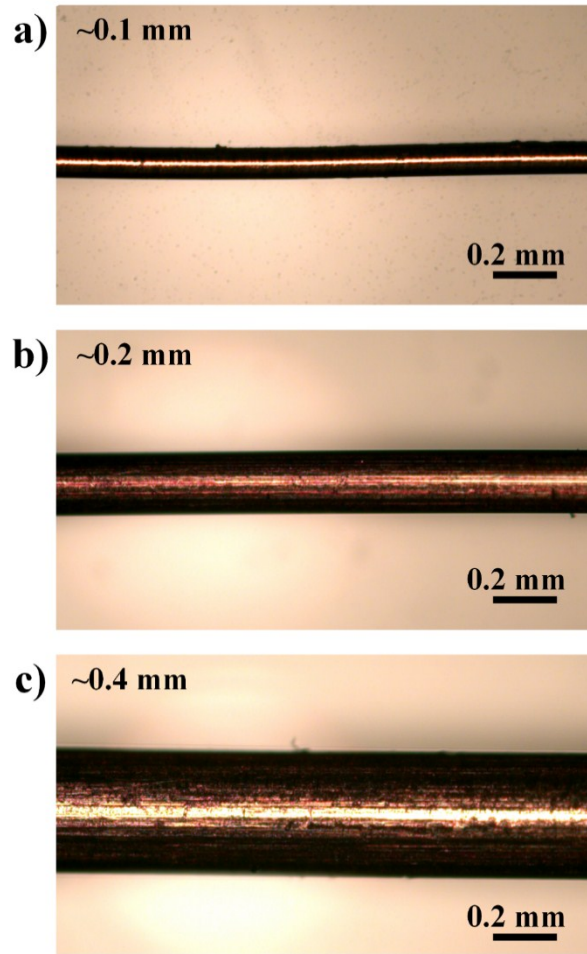


**Figure S1.** Microscopically optical images of commercial copper wires with a diameter of (a) 0.1 mm, (b) 0.2 mm and (c) 0.4 mm. Thick copper wires are mechanically strong and difficult to deform.

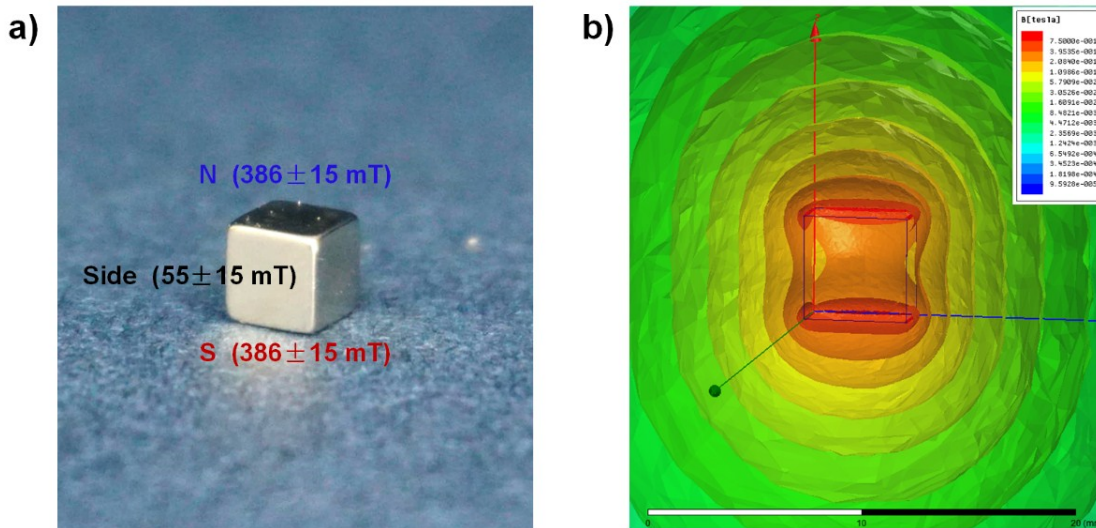


**Figure S2.** An NdFeB cubic magnet and its magnetic intensity distribution. (a) Optical photograph of a  $5 \times 5 \times 5 \text{ mm}^3$  NdFeB magnetic cube. The magnetic intensities on its north (N) pole, south (S) pole and sides has been investigated *via* a gaussmeter testing. (b) 3D calculated distribution of magnetic intensity of the magnetic cube. The strongest magnetic intensity (red area) exists in the N and S poles of the magnet.

## **Note S1. Detailed simulation results of magnetic flux when compressed in the vertical direction**

The ANSYS MAXWELL finite element analysis software was used to conduct two-dimensional (2D) and three-dimensional (3D) modeling of an NdFeB permanent magnet involved with a copper helix. The 2D simulation modeling was employed a static magnetic field solver with horizontal X-axis and vertical Y-axis. The permanent magnet was set as a cube of  $5 \text{ mm} \times 5 \text{ mm} \times 5 \text{ mm}$ , followed by magnetizing in the direction of positive Y axis (the top for N pole and the bottom for S pole) according to NdFeB parameters. In this work, setting magnetic coercivity of  $H_c = -905000 \text{ A/m}$ , as well as residual flux density of  $B_r = 1.13668 \text{ T}$ . The helix involved in experiments was equivalent to parallel rings with the same horizontal diameter and number. 8-layered copper helix has been equivalent with the same number of parallel rings (see black dot lines in Figure 2d of manuscript) for simplified calculation.

In the simulation process, we assume the following conditions:

- (1) 8-layered copper helix is equivalent with the same number of parallel rings;
- (2) The equivalent ring is a coaxial ring;
- (3) The helix is in an infinite vacuum.

Thus, the calculated distribution of magnetic intensity was shown in **Figure S3**.

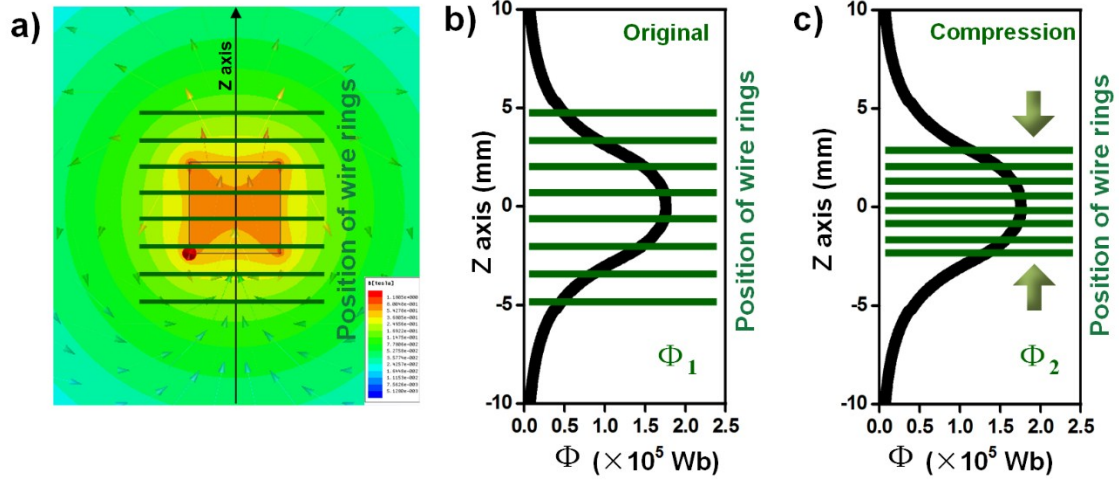


**Figure S3.** Calculated the total magnetic flux of a magnetoelastic elastomer cube before/after compression. (a) 2D calculated distribution (x-z plane) of magnetic intensity inside the elastomer. Green lines in (a) represent the positioning of 8 equivalent rings. The arrow indicates the direction of magnetic field from S to N pole. The dependence of magnetic flux on the Z-axis distance (b) before and (c) after the compression according to the calculated result of (a).

According to Faraday's law of electromagnetic induction:

$$E = \frac{\Delta\Phi}{\Delta t} \quad (\text{S1})$$

Where  $E$  is the induced electromotive force,  $\Delta\Phi$  is the total amount of change in magnetic flux, and  $\Delta t$  is the compression time.

$$\Delta\Phi = \Phi_{\text{II}} - \Phi_{\text{I}} \quad (\text{S2})$$

$$\Delta t = t_2 - t_1 \quad (\text{S3})$$

Where  $\Phi_{\text{II}}$  is the total magnetic flux after the helix is compressed,  $\Phi_{\text{I}}$  is the total magnetic flux when the helix is in original or recovered status;  $t_2$  is the moment after the helix has been compressed, and  $t_1$  is the moment when the helix just begins to compress.

Since the distribution of magnetic intensity is not uniform around the magnet, the calculation of the magnetic flux through one ring is as below:

$$\Phi_i = \int_{S_i} \vec{B} \cdot \vec{S} \quad (\text{S4})$$

Where  $\vec{B}$  is the vector form of the magnetic intensity,  $\vec{S}$  is the vector form of area of the ring, and n is the number of rings.

Then, the total magnetic flux of helix before/after the compression can be calculated as below:

$$\Phi_{\text{II}} = \sum_{i=1}^n \Phi_i \quad (\text{S5})$$

$$\Phi_{\text{I}} = \sum_{i=1}^n \Phi_i \quad (\text{S6})$$

According to **Figure S3b** and **3c**, the positions of the rings in **equation S5** and **S6** are different caused by the compression, resulting in diverse magnetic fluxes (see **Table S1**). Where  $\Phi_i$  can be calculated in the field calculator of post-processing in Maxwell software.

**Table S1.** Calculated total magnetic flux of helix before/after a vertical compression

Total magnetic flux before compression ( $\times 10^{-5}$ Wb)	Total magnetic flux after compression ( $\times 10^{-5}$ Wb)	The change of magnetic flux ( $\times 10^{-5}$ Wb)
8.3	11.7	3.4

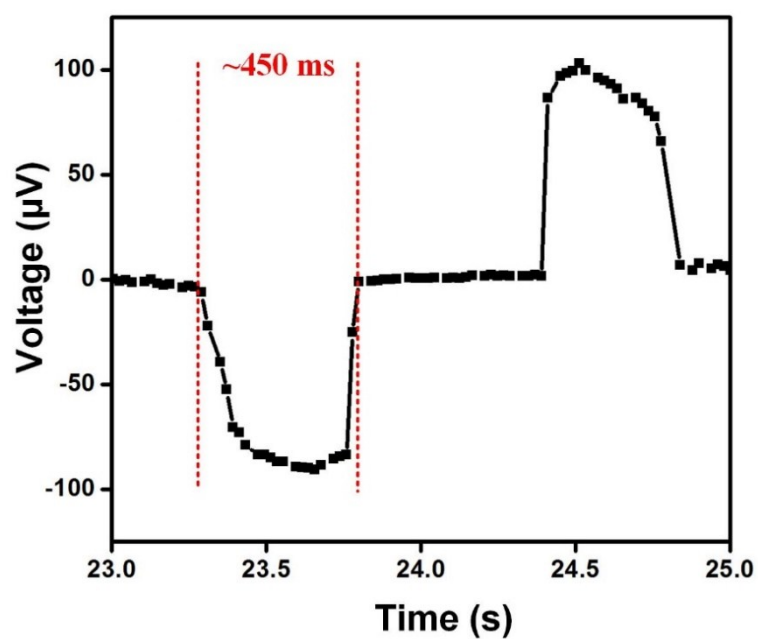


**Figure S4.** Single-cycle response of the magnetolectric elastomer, which exhibits a compression time of 450 ms. The applied pressure strain was 55%, the compression speed was set at 800 mm/min and under the room temperature.

## Note S2. Detailed simulation results of magnetic flux when compressed in the horizontal direction

Different from being compressed in the vertical direction, the copper helix in the magnetoelectric elastomer only changed its ring shape in the x-y plane (see **Figure S5**) when compressed in the horizontal direction.

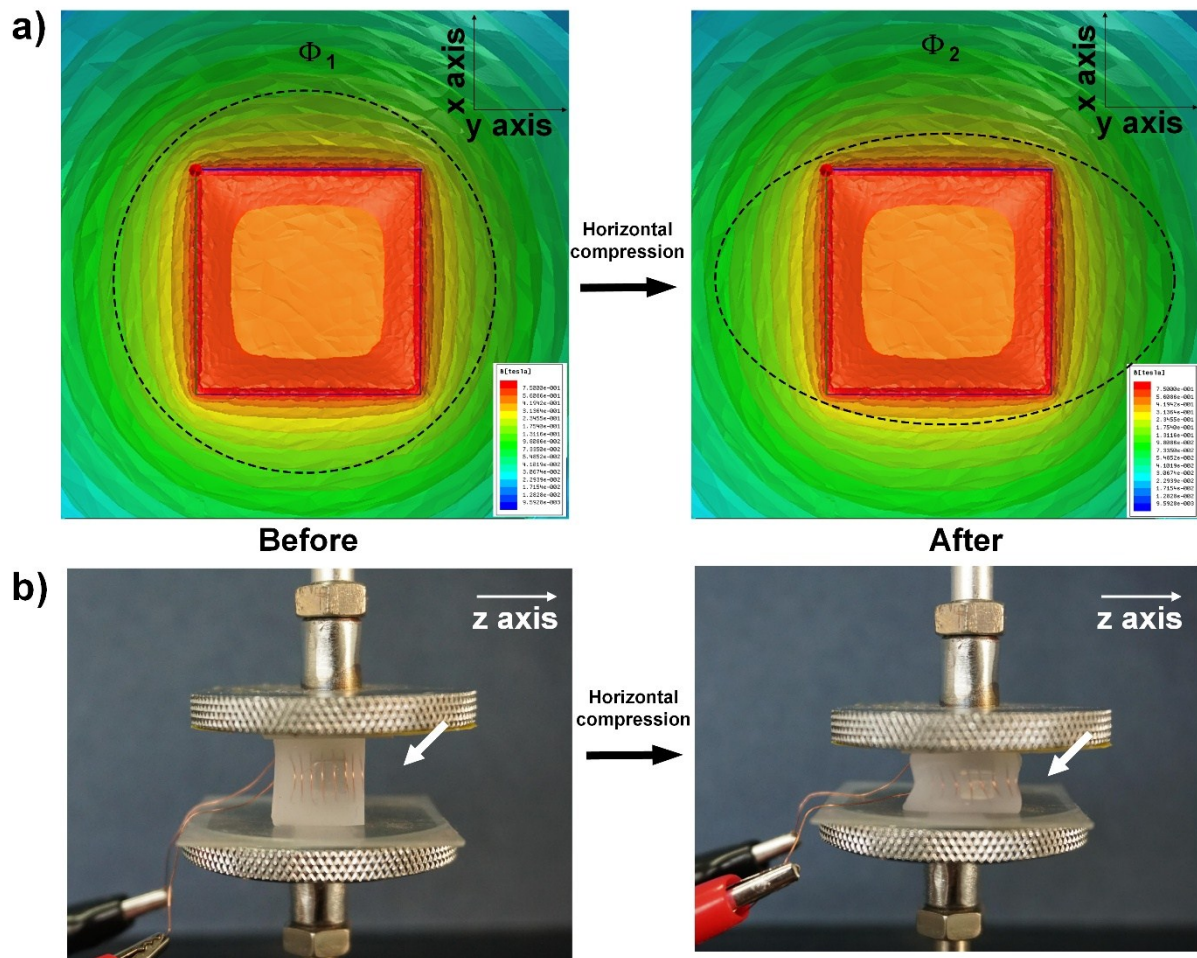


**Figure S5.** a) Calculated 2D distribution (x-y plane) and b) Photographs of a magnetoelectric elastomer before/after a horizontal compression.

A horizontal compression not only change the cross-sectional area from a circle to an ellipse shape but also enlarge the distance between the rings of copper helix along Z-axis (Figure S5b). In this case, the calculation of the magnetic flux through the rings is as below:



$$E(V) = -N \cdot \frac{\Delta\Phi}{\Delta t} = -\sum_{i=1}^8 \frac{\Delta\Phi_i}{\Delta t} = -\sum_{i=1}^8 \frac{\Phi_i(after) - \Phi_i(before)}{\Delta t} \quad (S7)$$

The  $\Phi_i$  (before) and  $\Phi_i$  (after) can be calculated according to equation S4. The result of total magnetic fluxes can be found in Table S2.

**Table S2.** Calculated magnetic flux of helix before/after a horizontal compression

Total magnetic flux before compression ( $\times 10^{-5}$ Wb)	Total magnetic flux after compression ( $\times 10^{-5}$ Wb)	The change of magnetic flux ( $\times 10^{-5}$ Wb)
8.3	6.9	-1.4

### Note S3. Detailed simulation results of magnetic flux of samples with different relative positions between the magnet and the helix

The relative position between the copper helix (electrical part) and the magnet (magnetic part) greatly affect the output performance of magnetoelectric elastomers. Two other samples, one magnetoelectric elastomer fixed the magnet cube above the copper helix top (labeled as HUST-1b, **Figure S6a**) while the other one kept the top edges of magnet cube and the copper helix at the same level (labeled as HUST-1c, **Figure S6d**), were fabricated. The calculated distribution of magnetic intensity was shown in **Figure S6**.

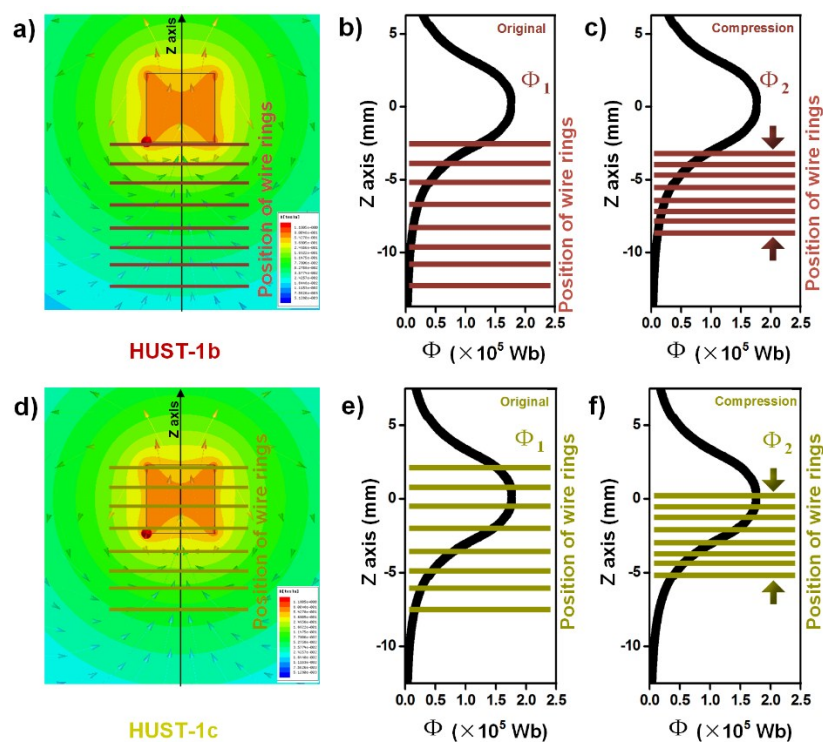


**Figure S6.** Calculated the total magnetic flux of two other magnetoelectric elastomer cubes before/after pressure. (a), (d) are 2D calculated distributions (x-z plane) of magnetic intensity inside these two elastomers. Brown and yellow lines in (a,d) represent the positioning of 8 equivalent rings. The arrow indicates the direction of magnetic field from S to N pole. The dependence of magnetic fluxes on the Z-axis distance (b,e) before and (c,f) after the compression according to the calculated result of (a,d), respectively.

According to **Figure S6**, the positions of the rings in the equations S4-S6 are different caused by the compression, resulting in diverse magnetic fluxes (see **Table S3**). Where  $\Phi_i$  can be calculated in the field calculator of post-processing in Maxwell software.

**Table S3.** Calculated total magnetic flux of other two samples before/after a vertical compression

Sample	Total magnetic flux before compression ( $\times 10^{-5}$ Wb)	Total magnetic flux after compression ( $\times 10^{-5}$ Wb)	The change of magnetic flux ( $\times 10^{-5}$ Wb)
HUST-1b	2.4	3.9	1.5
HUST-1c	8.5	10.6	2.1

These calculations are consistent with the experiment results (see **Figure 3k** of the manuscript).

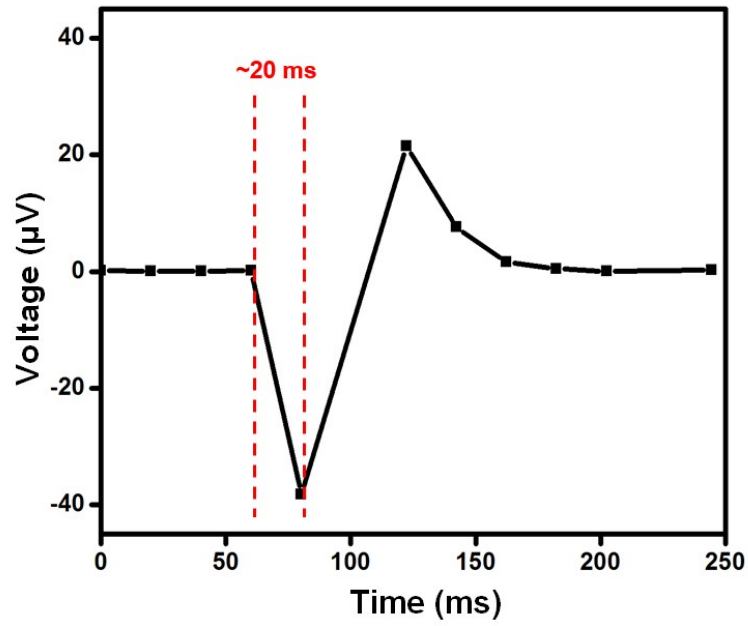


**Figure S7.** Instant response of an optimal magnetolectric elastomer, which exhibits a response time down to 20 ms via a finger tapping at the frequency of  $\sim 4$  Hz.

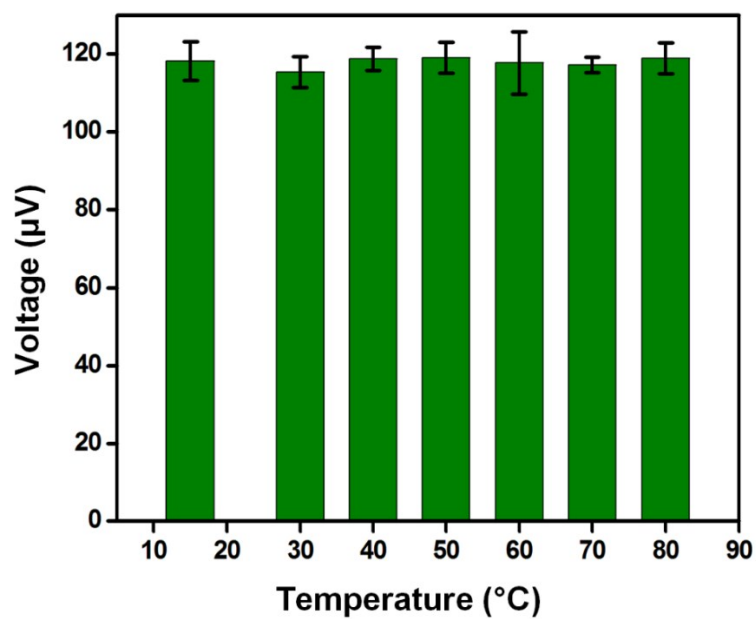


**Figure S8.** A resistance of the magnetolectric elastomer to the temperature. Electric response of the electromagnetic elastomer under various ambient temperature. The voltage showed a stable performance without any obvious fluctuation from 15 °C to 80 °C.

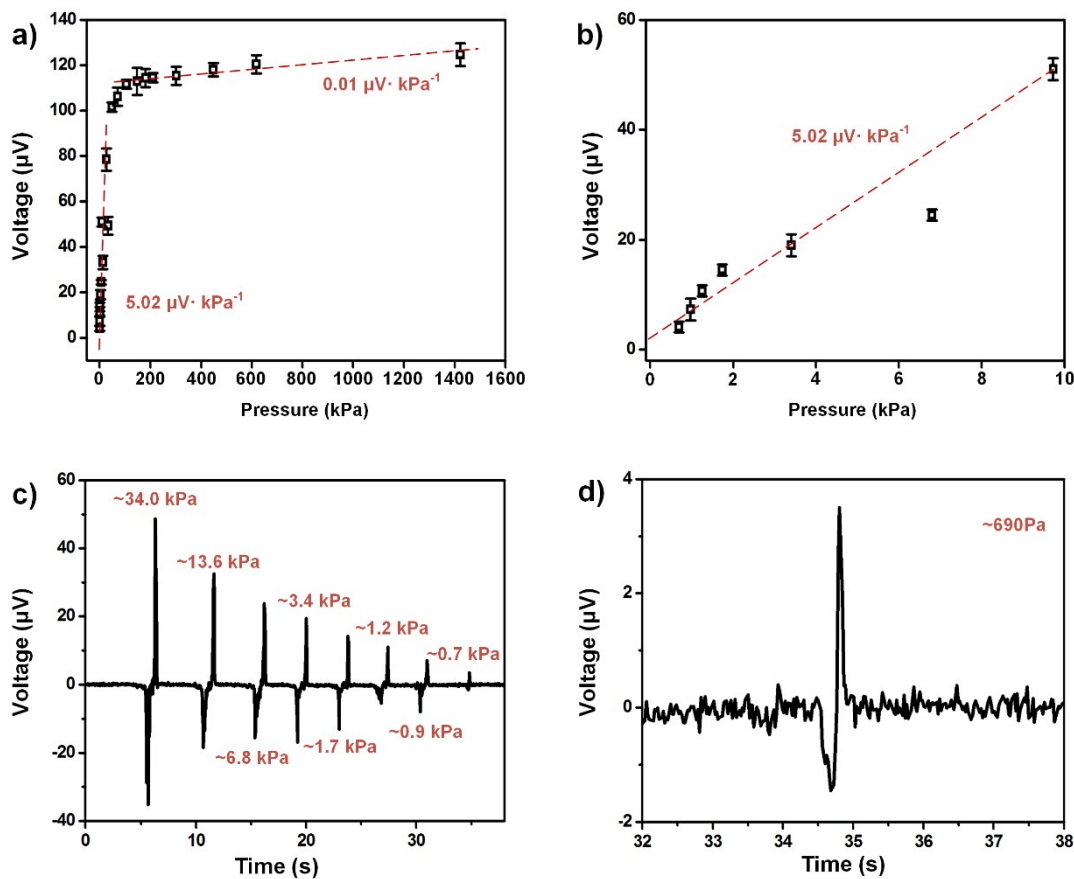


**Figure S9.** Pressure response of the magnetoelectric elastomer as a tactile sensor. (a) Pressure-voltage correlation of the elastomer. (b) Magnified images of pressure-response plots for the electromagnetic elastomer ranging from (a) 0-10 kPa. (c) Output voltage of the elastomer measured under a series of low pressures. (d) The minimum pressure response of the elastomer base sensor is around 690 Pa. Note: (a,b) was investigated using a programmed compression machine. In this case, the compression speed can be fixed at 800 mm/min. (c,d) was tested by manually adding different weights. Thus, the compression speed was quicker than the counterpart by the compression machine.

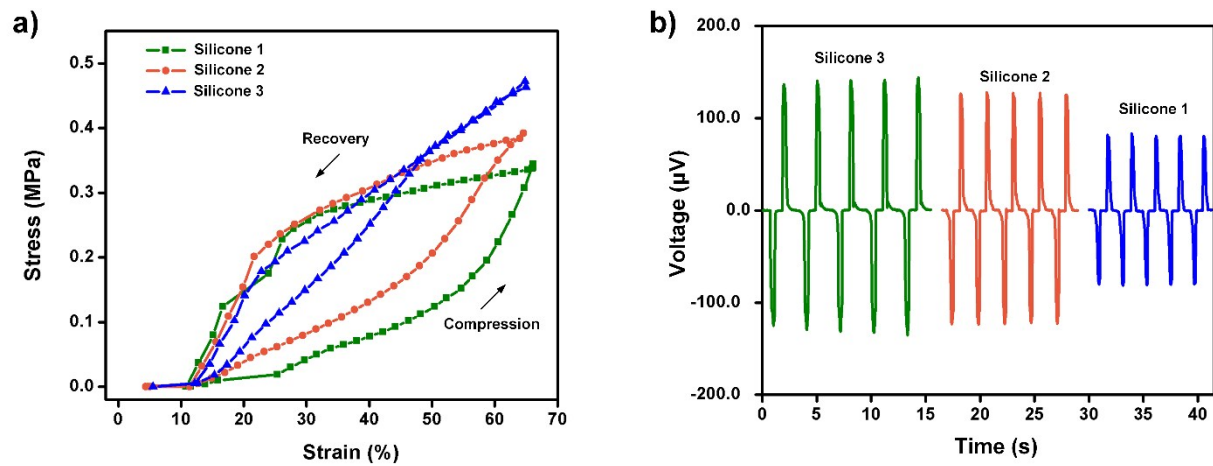


**Figure S10.** The dependence of the output voltage on the stiffness of silicone elastomers. (a) The correlation of stress and strain for a magnetoelastic elastomer in one cycle at a set compressing speed of 800 mm/min. Three kinds of silicone elastomers were tested, showing diverse stiffness. (b) Electric response of the electromagnetic elastomers under the same stress loading (0.1 MPa). The softest silicone elastomers contributed to the largest output voltages.